Organic Electronics 52 (2018) 350–355

Contents lists available at ScienceDirect

Organic Electronics

journal homepage: www.elsevier.com/locate/orgel

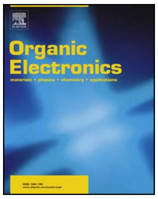

On the performance of polymer:organometal halide perovskite composite light emitting devices: The effects of polymer additives

Xiaxia Ji, Xuefeng Peng, Qi Wang, Jie Ren, Zuhong Xiong, Xiaohui Yang*

School of Physical Science and Technology, Southwest University, Chongqing 400715, PR China

ARTICLE INFO

Keywords:
Polymer:organometallic halide perovskite composites
Polymer additive
Light emitting devices
Charge balance

ABSTRACT

The formation of the polymer:organometallic halide perovskite composites serves as a convenient and effective means to improve the morphology homogeneity of spin-coated perovskite films. Herein, we report the morphology, crystal structure and optoelectronic properties of the polymer:perovskite composites with a new polyacrylonitrile additive and make a direct comparison of the tributes with those of the widely-practiced poly(ethylene oxide) analogue. The results indicate the charge balance of light emitting devices depends on the polymer additive, which may relate to the extent of ion accumulation at the polymer:perovskite layer/hole injection layer interface.

1. Introduction

Organometallic halide perovskites (OHPs) are emerging as a new class of semiconducting materials due to the enticing properties such as solution-processability, low bulk trap densities, high absorption coefficients and long-range charge carrier diffusion lengths [1–3]. OHP light emitting devices (LEDs) have been widely studied for potential applications on the flat-panel displays since the prototype room-temperature operating devices were reported in 2014 [4]. Notable progress has been made on device performance through the simultaneous work of morphology control, composition manipulation and interfacial engineering [5,6]. To date, Huang et al. [7] reported the near-infrared OHP LEDs with the maximum external quantum efficiency (EQE) of 11.7% by exploiting the energy/charge funneling process among various layered OHP phases in a quasi-2D OHP emission layer (EML).

The effective control of OHP morphology is of the crucial importance for the development of high-performance OHP LEDs [8–12]. Several methods such as anti-solvent aided fast crystallization [13,14], the utilization of a hydrohalide acid additive [15], the manipulation of the ratio of the organic to inorganic compounds in the precursor [16,17] and the formation of the polymer:OHP composites [18–22] have been adopted to improve the homogeneity and surface coverage of OHP films. The addition of a polymer additive hinders the OHP diffusivity during the film drying stage and as a result inhibits the OHP crystal growth, serving as a straightforward, convenient and effective method to control OHP morphology [18–22]. Li et al. [18] reported the significant improvement of the morphology homogeneity and integrity of the $MAPbBr_3$ layers upon the incorporation of a polyimide precursor dielectric (PIP) additive and the related multilayer LEDs with high EQE of 1.2%. Single-layer LEDs using a composite EML of $MAPbBr_3$ and poly(ethylene oxide) (PEO) showed the EQE of 0.16%, where PEO had the important effects on improving the surface coverage and enhancing the ionic conductivity of the EML [19]. In a subsequent study, we reported the multilayer PEO:$MAPbBr_3$ LEDs with the maximum EQE of ca. 4% and the power efficiency (PE) of 7.6 lm/W [20]. Other polymers or macromolecules such as poly(2-ethyl-2-oxazoline) [23] and polyhedral oligomeric silsesquioxane [24] have also been used as the additives to prepare OHP LEDs. Masi et al. [22] conducted a comparative study on the influence of various polymer additives including poly[2-methoxy-5-(2-ethylhexyloxy)-1,4-phenylenevinylene] (MEH-PPV), poly(methyl methacrylate) (PMMA), poly[(9,9-bis(3′-(*N*,*N*-dimethylamino)propyl)-2,7-fluorene)-alt-2,7(9,9-dioctylfluorene)] (PFN), 2,4-dimethyl-poly(triarylamine) (PTAA), and polystyrene (PS) on the morphology of the resultant polymer:OHP composite layers and proposed that the various strengths of hydrogen bonds between the polymer additives and methylammonium cations (MA^+) caused different morphologies. Besides the morphology, the utilization of different polymer additives affects the optoelectronic properties of the OHP layers as well. Li et al. [19] correlated the EQE of the polymer:OHP composite LEDs with the ion conductivity of the polymer additive. Understanding the functionality of polymer additives is important for the further enhancement of the performance of the polymer:OHP composite LEDs. However, there are limited studies making a detailed comparison of the properties of various polymer:OHP composites to understand the effects of the polymer additive.

In this work, we report the morphology, crystallinity, photophysics

---

* Corresponding author.
E-mail address: xhyang@swu.edu.cn (X. Yang).

https://doi.org/10.1016/j.orgel.2017.11.026
Received 21 October 2017; Received in revised form 20 November 2017; Accepted 20 November 2017

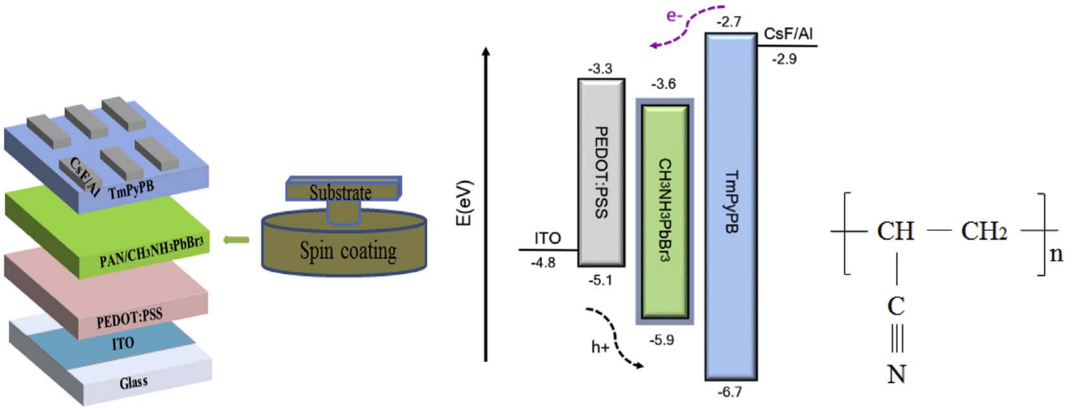

Scheme 1. Schematic architecture (a) and flat-band energy-level diagram (b) of the polymer:$CH_3NH_3PbBr_3$ devices; chemical structure of PAN (c).

and in particular the optoelectronic properties of the polyacrylonitrile (PAN):$MAPbBr_3$ composites. A direct comparison of the properties of the polymer:$MAPbBr_3$ composites with PAN and PEO indicates that the polymer additive plays a key role in determining the charge balance of the related LEDs.

2. Experimental section

Scheme 1 shows the configuration and energy level diagram of the polymer:$CH_3NH_3PbBr_3$ composite LEDs, where the energy levels of organic materials and $CH_3NH_3PbBr_3$ as well as the work-function of electrodes have been cited from the literature [25,26]. In the devices, the PAN(PEO):$CH_3NH_3PbBr_3$ composites served as EMLs, poly(3,4-ethylenedioxythiophene):poly(styrenesulfonate) (PEDOT:PSS) and cesium fluoride (CsF) functioned as hole injection and electron injection layer. 1,3,5-Tri(*m*-pyrid-3-yl-phenyl)benzene (TmPyPB) was employed as electron-transporting/hole-blocking layer. ITO and Al were the anode and cathode, respectively.

Methylammonium bromide (CH_3NH_3Br), lead(II) bromide ($PbBr_2$) and TmPyPB were purchased from Xi'an Polymer Technology Corporation. PEDOT:PSS (AI 4083) and PAN were obtained from Heraeus Corporation and Sigma-Aldrich, respectively. All of the materials were used as received. The $CH_3NH_3PbBr_3$ precursor solution was prepared by codissolving CH_3NH_3Br and $PbBr_2$ with a 2:1 M ratio in the anhydrous dimethyl sulphoxide (DMSO) and PAN was dissolved in DMSO as well. The $CH_3NH_3PbBr_3$ precursor and PAN solutions were heated and stirred at 60 °C for 12 h, afterward were mixed with the respective PAN:$CH_3NH_3PbBr_3$ weight ratio of 0.25:1, 0.5:1, 0.75:1 and 1:1. The PAN:$CH_3NH_3PbBr_3$ solutions were heated and stirred at 60 °C for 2 h before use. Pre-cleaned indium tin oxide (ITO)-coated glass substrates were UV-ozone treated for 20 min immediately prior to device preparation. A PEDOT:PSS layer was spin-coated onto the ITO substrates, which was thermally treated at 170 °C for 10 min under the ambient conditions to remove the moisture. The samples were transferred into a nitrogen-filled glovebox with the oxygen and moisture levels both at ca. 1 ppm. A PAN:$CH_3NH_3Br_3$ EML was deposited onto the PEDOT:PSS layer from the DMSO solution, which was thermally treated at 100 °C for 30 min. The thickness of the respective PEDOT:PSS and PAN:$CH_3NH_3PbBr_3$ layer was ca. 70 and 50 nm as measured by a Dektak 6M stylus profilometer. Finally, 60 nm TmPyPB, 1 nm CsF and 100 nm aluminum (Al) were sequentially deposited by vacuum evaporation. The preparation of the PEO:$CH_3NH_3PbBr_3$ devices was referred to our previous work [20]. The active area of the devices was 0.18 cm^2. The devices were encapsulated with a glass lid using a UV-curable resin before testing.

For the preparation of the hole-dominated devices, 20 nm 1,3-bis (9H-carbazol-9-yl)benzene(mCP), 10 nm MoO_3 and 100 nm Al were thermally deposited onto the polymer:$CH_3NH_3PbBr_3$ layers in sequence. A polymer:$CH_3NH_3PbBr_3$ layer was spin-coated onto the polyethyleneimine ethoxylated (PEIE) modified ZnO layer for the preparation of the electron-dominated devices [27]. The other layers were prepared in the same manner as stated above for the LEDs.

The voltage – current density – luminance (V – I – L) characteristics of the devices were measured by a programmed Keithley 2400 Source – Meter and Konica – Minolta CS – 100A Chroma Meter. The electroluminescent (EL) spectra were recorded with an Ocean Optics USB4000 UV–Vis spectrometer. The photoluminescence (PL) spectra were obtained by using an Edinburgh FLS920 steady-state fluorescence spectrometer. The structure analysis of the polymer:$CH_3NH_3PbBr_3$ films was conducted with a Rigaku D/Max-B X-ray diffractometer (XRD) equipped with Cu Kα radiation source. The morphology of the polymer:$CH_3NH_3PbBr_3$ films was studied using a Jeon scanning electron microscope (SEM). The Fourier transform infrared (FT-IR) spectra were obtained with an IR – 211 infrared spectrometer. All of the measurements were carried out at room temperature under the ambient conditions.

3. Results and discussion

Polyacrylonitrile (PAN) shows large mechanical strength and high stability toward the oxygen and moisture in the ambient conditions. The utilization of PAN additive is expected to ameliorate the mechanical property and environmental stability of the OHP materials. PAN shows the large band-gap energy of 2.57 eV [28] and low electrical conductivity of $< 10^{-12}$ S/cm [29], therefore, PAN is not involved in the charge injection and transport processes of the devices. Fig. 1 shows the top-view SEM images of the PAN:$CH_3NH_3PbBr_3$ samples with various PAN contents. All of the samples show continuous crystalline morphologies with few pores and voids. PAN on one hand decreases the OHP diffusivity during the film forming process, on the other hand it works as a scaffold to adjust the OHP crystal growth [19,30]. Some $CH_3NH_3PbBr_3$ crystals can be found in the SEM image of the 0.25:1 sample. With increasing PAN proportion, the size of $CH_3NH_3PbBr_3$ crystals is reduced and the homogeneity of the samples is improved, which is beneficial for the reduction of the leakage current and the formation of good contacts with the adjacent charge transporting layers. Similar evolution of the surface morphology with the changes of the $CH_3NH_3PbBr_3$ contents for the PEO:$CH_3NH_3PbBr_3$ samples was reported [20]. The SEM image of the PEO:$CH_3NH_3PbBr_3$ sample with the PEO:$CH_3NH_3PbBr_3$ ratio of 0.5:1 is presented in the inset of Fig. 1b as well. It can be seen that $CH_3NH_3PbBr_3$ grain size of the PAN:$CH_3NH_3PbBr_3$ samples is smaller than that of the PEO:$CH_3NH_3PbBr_3$ analogue.

We have carried out the XRD measurements to study the composition and crystal structure of the PAN:$CH_3NH_3PbBr_3$ films. As shown in Fig. 2, the XRD patterns of the samples show the peaks at 14.9, 21.2,